

---

# PIVEN: A Deep Neural Network for Prediction Intervals with Specific Value Prediction

---

**Eli Simhayev**  
Ben-Gurion University of the Negev  
Beer-Sheva, Israel  
elisim@post.bgu.ac.il

**Gilad Katz**  
Ben-Gurion University of the Negev  
Beer-Sheva, Israel  
giladkz@post.bgu.ac.il

**Lior Rokach**  
Ben-Gurion University of the Negev  
Beer-Sheva, Israel  
liorrk@post.bgu.ac.il

## Abstract

Improving the robustness of neural nets in regression tasks is key to their application in multiple domains. Deep learning-based approaches aim to achieve this goal either by improving their prediction of specific values (i.e., point prediction), or by producing prediction intervals (PIs) that quantify uncertainty. We present PIVEN, a deep neural network for producing both a PI and a value prediction. Our loss function expresses the value prediction as a function of the upper and lower bounds, thus ensuring that it falls within the interval without increasing model complexity. Moreover, our approach makes no assumptions regarding data distribution within the PI, making its value prediction more effective for various real-world problems. Experiments and ablation tests on known benchmarks show that our approach produces tighter uncertainty bounds than the current state-of-the-art approaches for producing PIs, while maintaining comparable performance to the state-of-the-art approach for value-prediction. Additionally, we go beyond previous work and include large image datasets in our evaluation, where PIVEN is combined with modern neural nets.

## 1 Introduction

Deep neural networks (DNNs) have been achieving state-of-the-art results in a large variety of complex problems. These include automated decision making and recommendation in the medical domain [26], autonomous drones [11] and self driving cars [2]. In many of these domains, it is crucial not only that the prediction made by the DNN is accurate, but rather that its uncertainty is quantified. Quantifying uncertainty has many benefits, including risk reduction and more reliable planning [14]. In regression, uncertainty is quantified using prediction intervals (PIs), which offer upper and lower bounds on the value of a data point for a given probability (e.g., 95%). Existing non-Bayesian PI generation methods can be roughly divided into two groups: *a*) performing multiple runs of the regression problem, as in dropout [3] or ensemble-based methods [17], then deriving post-hoc the PI from prediction variance, and; *b*) dedicated architectures for the PI generation [23, 32, 29].

While effective, both approaches have shortcomings. The former group is not optimized for PIs generation, having to convert a set of sampled values into a distribution. This lack of PI optimization makes using these approaches difficult in domains such as financial risk mitigation or scheduling. For example, providing a PI for the number of days a machine can function without malfunctioning (e.g., 30-45 days with 99% certainty) is more valuable than a prediction for the specific time of failure.

The latter group—PI-dedicated architectures—provides accurate upper and lower bounds for the prediction, but finds it difficult to produce accurate value predictions. One approach for producing values is to select the middle of the interval [23, 32], but this often leads to sub-optimal results due to various implicit assumptions regarding data distribution within the PI. Another recent approach [29] attempts to learn the value prediction simultaneously by adding terms to the loss function. While effective, the additional terms increase model complexity, consequently requiring heavy optimization.

We propose PIVEN (**p**rediction **i**ntervals with **s**pecific **v**alue **p**rediction), a novel approach for simultaneous PI generation and value prediction using DNNs. Our approach combines the benefits of the two above-mentioned groups by producing *both* a PI and a value prediction, while ensuring that the latter is within the former. By doing so, PIVEN ensures prediction integrity, without increasing model complexity. We follow the experimental procedure of recent works, and compare our approach to current best-performing methods: *a*) Quality-Driven PI (QD) [23], a dedicated PI generation method; *b*) QD-Plus [29], a recent improvement of QD which adds additional terms for the value prediction, and; *c*) Deep Ensembles (DE) [17]. Our results show that PIVEN outperforms QD and QD-Plus by producing narrower PIs, while simultaneously achieving comparable results to DE in terms of value prediction. We are also the first to include large image datasets and explore the integration of our PI-producing methods with large convolutional architecture.

## 2 Related Work

Modeling uncertainty in deep learning has been an active area of research in recent years [23, 25, 3, 17, 13, 12, 4, 22, 36]. Studies in uncertainty modeling and regression can be generally divided into two groups: *PI-based* and *non-PI-based*. Non-PI approaches utilize both Bayesian [18] and non-Bayesian approaches. The former methods define a prior distribution on the weights and biases of a neural net (NN), while inferring a posterior distribution from the training data. Non-Bayesian methods [3, 17, 25] do not use initial prior distributions. In [3], Monte Carlo sampling was used to estimate the predictive uncertainty of NNs through the use of dropout over multiple runs. A later study [17] employed a combination of ensemble learning and adversarial training to quantify model uncertainty. In an expansion of a previously-proposed approach [20], each NN was optimized to learn the mean and variance of the data, assuming a Gaussian distribution. Recently, [25] proposed a post-hoc procedure using Gaussian processes to measure uncertainty.

PI-based approaches are designed to produce a PI for each sample. [13] propose a post-processing approach that considers the regression problem as one of classification, and uses the output of the final softmax layer to produce PIs. [32] propose the use of a loss function designed to learn all conditional quantiles of a given target variable. LUBE [14] consists of a loss function optimized for the creation of PIs, but has the caveat of not being able to use stochastic gradient descent (SGD) for its optimization. A recent study [23] inspired by LUBE, proposed a loss function that is both optimized for the generation of PIs and can be optimized using SGD. Recently, [29] proposed a method for combining PI generation and value prediction, but the approach requires computationally-heavy post-hoc optimization.

The two groups presented above tends to under-perform when applied to tasks for which its loss function was not optimized: Non-PI approaches produce more accurate value predictions, but are not optimized to produce PI and therefore produce bounds that are less tight. PI-based methods produce tight bounds, but tend to underperform when producing value predictions. Several recent studies attempted to produce both value predictions and PIs: [16, 27] do so by using conformal prediction with quantile regression, while QD+ [29] simultaneously outputs a PI and a value prediction using an additional output. While effective, these approaches require either a complex splitting strategy [16, 27], or the addition of multiple terms to the loss function, consequently increasing model complexity and requiring computationally heavy post-hoc optimization. Contrary to these approaches, PIVEN produces PIs with value predictions by using a novel loss function and without any increases in complexity.

### 3 Motivation

#### 3.1 Problem Formulation

We consider a NN regressor that processes an input  $x \in \mathcal{X}$  with an associated label  $y \in \mathbb{R}$ , where  $\mathcal{X}$  can be any feature space (e.g., tabular data, age prediction from images). Let  $(x_i, y_i) \in \mathcal{X} \times \mathbb{R}$  be a data point along with its target value. Let  $U_i$  and  $L_i$  be the upper and lower bounds of PIs corresponding to the  $i$ th sample. Our goal is to construct  $(L_i, U_i, y_i)$  so that  $\Pr(L_i \leq y_i \leq U_i) \geq 1 - \alpha$ . We refer to  $1 - \alpha$  as the confidence level of the PI.

We define two quantitative measures (Eq. 1 and 2) for PIs evaluation (see [14]). When combined, these metrics enable us to comprehensively evaluate the quality of generated PIs. *Coverage* is the ratio of dataset samples that fall within their respective PIs, measured using the *prediction interval coverage probability* (PICP) metric. The variable  $n$  denotes the number of samples and  $k_i = 1$  if  $y_i \in (L_i, U_i)$ , otherwise  $k_i = 0$ . *Mean prediction interval width* (MPIW) is a quality metric for the generated PIs whose goal is producing as tight a bound as possible.

$$PICP := \frac{1}{n} \sum_{i=1}^n k_i \quad (1) \quad MPIW := \frac{1}{n} \sum_{i=1}^n U_i - L_i \quad (2)$$

#### 3.2 Motivation

PI-producing NNs aim to minimize PI width (MPIW) while maintaining predefined coverage (PICP). This approach has two significant drawbacks:

**Lack of value prediction capabilities.** Current PI-producing architectures do not output specific values (their original task). Most studies [23, 32] circumvent this problem by returning the middle of the PI, but this approach leads to sub-optimal results for skewed distributions. We are aware of only one previous study that aims to address this challenge [29], but it has shortcomings we discuss in our evaluation in Section 5.

**Overfitting.** The MPIW metric is optimized for the predefined percentage of samples that fall within their generated PIs (defined by PICP). As a result, the NN essentially overfits to a subset of the data.

PIVEN is specifically designed to address these shortcomings. First, our approach is the first to propose an integrated architecture capable of producing both PIs and well-calibrated value predictions in an end-to-end manner, without post-hoc optimization or increases to model complexity. Moreover, since our approach produces predictions for *all* training set samples, PIVEN does not overfit to data values which were contained in their respective PIs.

Secondly, PIVEN proposes a novel method for producing the value prediction. While previous studies either provided the middle of the PI [23, 32] or the mean-variance [17] as their value predictions, PIVEN’s auxiliary head can produce any value within the PI, while also being distribution free (i.e., without making any assumptions regarding data distribution within the PI). By expressing the value prediction as a function of the upper and lower bounds, we ensure that the prediction *always* falls within the PI without having to add additional penalty terms to the loss. Our use of a *non-Gaussian observation model* enables us to produce predictions that are not in the middle of the interval and create representations that are more characteristic of many real-world cases, where the values within the PI is not necessarily uniformly distributed (see Section 5.4).

## 4 Method

### 4.1 System Architecture

The proposed architecture is presented in Figure 1. It consists of three components:

**Backbone block.** The main body block, consisting of a varying number of DNN layers or sub-blocks. The goal of this component is to transform the input into a latent representation that is then provided as input to the other components. It is important to note that PIVEN supports any architecture type (e.g., dense, convolutions) that can be applied to a regression problem. Moreover, pre-trained

architectures can also be easily used, with PIVEN being added on top of the architecture for an additional short training. For example, we use pre-trained DenseNet architectures in our experiments.

**Upper & lower-bound heads.**  $L(x)$  and  $U(x)$  produce the lower and upper bounds of the PI respectively, such that  $\Pr(L(x) \leq y(x) \leq U(x)) \geq 1 - \alpha$  where  $y(x)$  is the value prediction and  $1 - \alpha$  is the predefined confidence level.

**Auxiliary head.** The auxiliary prediction head,  $v(x)$ , enables us to produce a value prediction.  $v(x)$  does not produce the value prediction directly, but rather produces the *relative weight that should be given to each of the two bounds*. We define the value prediction using,

$$y = v \cdot U + (1 - v) \cdot L \quad (3)$$

where  $v \in (0, 1)$ . Aside from enabling us to directly produce a value prediction, the auxiliary head has additional advantages in terms of optimization and the prevention of overfitting. We elaborate further in Section 4.3.

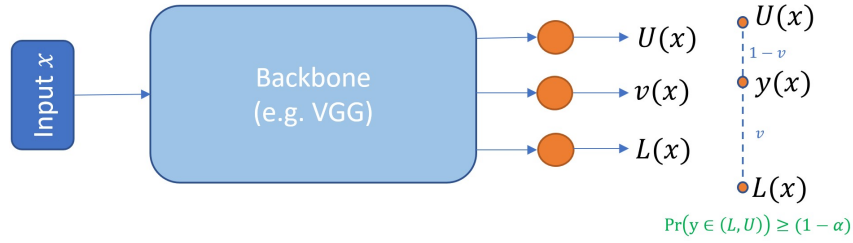


Figure 1: The PIVEN schematic architecture

## 4.2 Network Optimization

Our goal is to generate narrow PIs, measured by  $MPIW$ , while maintaining the desired level of coverage  $PICP = 1 - \alpha$ . However, PIs that fail to capture their respective data point should not be encouraged to shrink further. Therefore, we define *captured MPIW* ( $MPIW_{capt}$ ) as the  $MPIW$  of only those points for which  $L_i \leq y_i \leq U_i$ ,

$$MPIW_{capt} := \frac{1}{c} \sum_{i=1}^n (U_i - L_i) \cdot k_i \quad (4)$$

where  $c = \sum_{i=1}^n k_i$ . Hence, we seek to minimize  $MPIW_{capt}$  subject to  $PICP \geq 1 - \alpha$ :

$$\theta^* = \arg \min_{\theta} (MPIW_{capt, \theta}) \text{ s.t. } PICP_{\theta} \geq 1 - \alpha \quad (5)$$

where  $\theta$  is the parameters of the neural net. To enforce the coverage constraint, we utilize a variant of the well-known Interior Point Method (IPM) [24], resulting in an unconstrained loss:

$$\begin{aligned} \mathcal{L}_{PI} &= MPIW_{capt, \theta} + \sqrt{n} \cdot \lambda \Psi(1 - \alpha - PICP_{\theta}) \\ \Psi(x) &:= \max(0, x)^2 \end{aligned} \quad (6)$$

where  $\Psi$  is a quadratic penalty function,  $n$  is the batch size which was included because a larger sample size would increase confidence in the value of  $PICP$  (thus increasing the loss) and  $\lambda$  is a hyperparameter controlling the relative importance of width vs. coverage. We use a default value of  $\lambda = 15$  in all our experiments, and perform further analysis of this parameter in Section 6.2.

In practice, optimizing the loss with a discrete version of  $\mathbf{k}$  (see eq. 4) fails to converge, because the gradient is always positive for all possible values. We therefore define a continuous version of  $\mathbf{k}$ , denoted as  $\mathbf{k}_{soft} = \sigma(s \cdot (\mathbf{y} - \mathbf{L})) \odot \sigma(s \cdot (\mathbf{U} - \mathbf{y}))$ , where  $\sigma$  is the sigmoid function, and  $s > 0$  is a softening factor. The final version of  $\mathcal{L}_{PI}$  uses the continuous and discrete versions of  $\mathbf{k}$  in its calculations of the  $PICP$  and  $MPIW_{capt}$  metrics, respectively. The discrete  $\mathbf{k}$  enables us to assign a score of zero to points outside the interval, while  $\mathbf{k}_{soft}$  produces continuous values that enable gradient calculations.

### 4.3 The Auxiliary Head

The auxiliary head  $v(x)$  serves three goals: first, it enables PIVEN to select any point within the PI as the value prediction, an approach that produces superior results to choosing the middle of the PI, as done in previous works. Secondly, since we produce a value prediction for every point, and not only to those that fall within their PI, we enable PIVEN to learn from the entire dataset. By doing so we avoid the overfitting problem described in Section 3.1. Thirdly, the value prediction is expressed as a function of the upper and lower bounds, thus ensuring that all three outputs – upper, lower, and auxiliary – are optimized jointly. This setting also ensures the integrity of our output, since the value prediction *always* falls within the interval. To optimize the output of  $v(x)$ , we minimize:

$$\mathcal{L}_v = \frac{1}{n} \sum_{i=1}^n \ell(v_i \cdot U_i + (1 - v_i) \cdot L_i, y_i) \quad (7)$$

where  $\ell$  can be any regression objective against the ground-truth. Our final loss function is a convex combination of  $\mathcal{L}_{PI}$ , and the auxiliary loss  $\mathcal{L}_v$ . Thus, the overall training objective is:

$$\mathcal{L}_{PIVEN} = \beta \mathcal{L}_{PI} + (1 - \beta) \mathcal{L}_v \quad (8)$$

where  $\beta$  is a hyperparameter that balances the two goals of our approach: producing narrow PIs and accurate value predictions. In all our experiments, we chose to assign equal priorities to both goals by setting  $\beta = 0.5$ . An analysis of the effects of various values of  $\beta$  is presented in Section 6.2.

### 4.4 Using Ensembles to Estimate Model Uncertainty

Ensembles are commonly used to reduce uncertainty and improve performance. In our setting, each ensemble model produces a PI and a value prediction. These outputs need to be combined into a single PI and value prediction, thus capturing both the aleatoric and parametric uncertainties.

While PIs produced by a single PIVEN architecture could be used to capture aleatoric uncertainty, an ensemble of PIVEN architectures can capture the uncertainty of the PI itself. We consider the aggregation proposed by [17], as it is used by SOTA studies in the field:

Given an ensemble of  $m$  NNs trained with  $\mathcal{L}_{PIVEN}$ , let  $\tilde{U}$ ,  $\tilde{L}$  represent the PI, and  $\tilde{v}$ ,  $\tilde{y}$  represent the ensemble’s auxiliary and value prediction. We calculate the PI uncertainty and use the ensemble to generate the PIs and value predictions as follows:

$$\bar{U}_i = \frac{1}{m} \sum_{j=1}^m U_{ij} \quad (9) \quad \sigma_{PI}^2 = \sigma_{U_i}^2 = \frac{1}{m-1} \sum_{j=1}^m (U_{ij} - \bar{U}_i)^2 \quad (11)$$

$$\tilde{U}_i = \bar{U}_i + z_{\alpha/2} \cdot \sigma_{U_i} \quad (10) \quad \tilde{y}_i = \frac{1}{m} \sum_{j=1}^m v_{ij} \cdot U_{ij} + (1 - v_{ij}) \cdot L_{ij} \quad (12)$$

where  $(U_{ij}, L_{ij})$  and  $v_{ij}$  are the PI and the auxiliary prediction for data point  $i$ , for NN  $j$ . A similar procedure is done for  $\tilde{L}_i$ , subtracting  $z_{\alpha/2} \cdot \sigma_{L_i}$ , where  $z_{\alpha/2}$  is the Z score for confidence level  $1 - \alpha$ .

## 5 Evaluation

### 5.1 Baselines

We compare our performance to three top-performing baselines from recent years:

**Quality Driven PI (QD) [23].** QD produces PIs that minimize a smooth combination of the PICP/MPIW metrics without considering the value prediction task in its objective function. Its reported results make it state-of-the-art in terms of PI width and coverage.

**Quality Driven Plus (QD+) [29].** A recently proposed enhancement to QD, consisting of two improvements: *a)* additional terms to the loss functions, used to produce value predictions, and; *b)* a previously-proposed post-optimization aggregation method called SNM [33]. While effective, SNM has a very high computational overhead (as stated by the original authors [33]), which makes

QD+ impractical for large datasets such as our large image datasets, discussed in Section 5.2. We therefore run QD+ using the same optimization method as QD and PIVEN. This setting provides a level playing field and enables us to compare the performance of each method’s loss function, which is the main contribution of these respective studies. Nonetheless, for the sake of completeness, we also present all the reported results of the original QD+ algorithm together with our own experiments. These results, on the UCI datasets, are presented in Section 5.6.

**Deep Ensembles (DE) [17].** This work combines individual conditional Gaussian distribution with adversarial training, and uses the models’ variance to compute prediction intervals. Because DE outputs distributions instead of PIs, we first convert it to PIs, and then compute PICP and MPIW. DE’s reported results make one of the top performers with respect to value prediction.

## 5.2 The Evaluated Datasets

**Synthetic datasets.** We generate two datasets with skewed (i.e., neither Gaussian nor uniform) value distributions. We use these datasets to demonstrate PIVEN’s effectiveness compared to methods that only return the middle of the interval as a value prediction (namely, QD). Our datasets are the Sine and skewed-normal distributions.

**IMDB age estimation dataset.** The IMDB-WIKI dataset [28] is currently the largest age-labeled facial dataset available. Our dataset consists of 460,723 images from 20,284 celebrities, and the regression goal is to predict the age of the person in the image. This dataset is known to contain noise (i.e., aleatoric uncertainty), thus making it relevant (despite usually being used for pre-training).

**RSNA pediatric bone age dataset.** This dataset is a popular medical imaging dataset consisting of X-ray images of children’s hands [5]. The regression task is predicting one’s age from one’s bone image. The dataset contains 12,611 training images and 200 test set images.

**UCI Datasets.** A set of 10 datasets used by several state-of-the-art studies [3, 8, 17, 23]. Commonly used as benchmark for new studies.

Our selection of datasets is designed to achieve two goals: *a*) demonstrate that PIVEN is applicable to multiple and more challenging domains (e.g., images), unlike previous studies that were only applied to tabular datasets and; *b*) show that PIVEN significantly outperforms PI-based methods (5%–17% improvement in MPIW), while maintaining comparable performance to non-PI methods.

## 5.3 Experimental Setup

We evaluate all baselines using their reported deep architectures and hyperparameters. For full experimental details, please see Appendix A. We ran our experiments using a GPU server with two NVIDIA Tesla P100. Our code is implemented using TensorFlow [1], and is available online<sup>1</sup>.

**Synthetic datasets.** We used a neural net with one hidden layer of 100 nodes with ReLU [19]. All methods trained until convergence using the same initialization, loss and default hyperparameters:  $\alpha = 0.05$ ,  $\beta = 0.5$ ,  $\lambda = 15.0$ ,  $s = 160.0$ , with random seed set to 1. The generated data consisted of 100 points sampled from the interval  $[-2, 2]$ . We used  $\alpha = 100$  as the skewness parameter.

**IMDB age estimation dataset.** We use the DenseNet architecture [9] as the backbone block, then add two dense layers. We apply the data preprocessing used by [34]. We use 5-fold cross validation.

**RSNA bone age dataset.** We use VGG-16 [30] as the backbone block, with weights pre-trained on ImageNet. We add two convolutional layers followed by a dense layer, and perform additional training. This dataset has 200 predefined test images.

**UCI datasets.** We use the same experimental setup used by our baselines, as proposed by [8]. Results are averaged on 20 random 90%/10% splits of the data, except for the “Year Prediction MSD” and “Protein”, which were split once and five times respectively. Our network architecture is identical to that of our two baselines: one hidden layer with ReLU activation function, the Adam optimizer [15], and ensemble size  $M = 5$ . Input and target variables are normalized to zero mean and unit variance, like in previous works.

---

<sup>1</sup><https://github.com/anonymous/anonymous>

## 5.4 Synthetic Datasets: Value Prediction in Skewed Distributions

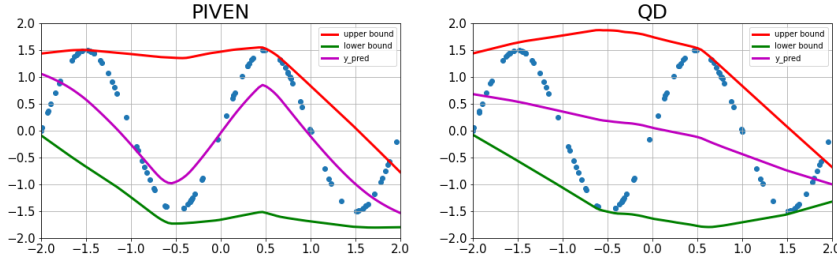


Figure 2: Comparison of value prediction for QD vs. PIVEN method, where  $y$  was generated by  $f(x) = 1.5 \sin(x)$ .

The goal of this evaluation is to demonstrate the shortcomings of returning the middle of the interval as value prediction, as done by methods such as QD. As noted in [23], QD “breaks the distribution-free assumption”, because such a selection is only optimal for Gaussian or uniformly based distributions. To test PIVEN’s ability to outperform QD in skewed distributions, we evaluate both approaches on the Sine and skewed-normal distributions. The results, presented in Figure 2 (for Sine) and in Figure 5 in the appendix (for skewed-normal), clearly illustrate PIVEN’s superior ability to adapt to multiple value distributions, through the use of its auxiliary head.

## 5.5 Large-Scale Image Datasets

Both bone age and IMDB are large and noisy image datasets. We follow [25] and add an additional baseline – denoted as NN – which is a single dense layer on top of existing architectures (DenseNet/VGG). This layer outputs value prediction using the MSE metric. Instead of RMSE, we use *mean absolute error* (MAE), which was the datasets’ chosen metric. For IMDB, it is clear that PIVEN outperforms the other PI-driven methods (QD and QD+) by wide margins—20% in MPIW and 43% in MAE—while also outperforming NN. DE performed best for this dataset, with a small margin over PIVEN, but this likely due to the fact that age distribution is a Gaussian, and therefore fully compatible with this baseline’s assumptions. PIVEN obtains comparable results to DE without relying on any distributional assumptions. It is also important to note that PIVEN performs significantly better when encountering outliers – very young or very old persons – as shown in Figure 13 in the appendix. In bone age, PIVEN outperforms all baselines in terms of MAE. Our approach fares slightly worse compared to QD on the MPIW metric, but that is likely due to its higher coverage (i.e., PICP), which means it had to contend with more samples, particularly those which were difficult to classify (the same applies for QD+, which likely contributed to its higher error rates).

Table 1: Results on the RSNA bone age and IMDB age estimation datasets.

Datasets	Method	PICP	MPIW	MAE
IMDB age	NN	NA	NA	7.08 ± 0.03
	QD	0.92 ± 0.01	3.47 ± 0.03	10.23 ± 0.12
	QD+	<b>1.00 ± 0.00</b>	5.01 ± 0.11	10.08 ± 0.03
	DE	<b>0.95 ± 0.01</b>	<b>2.61 ± 0.05</b>	<b>6.66 ± 0.06</b>
	PIVEN	<b>0.95 ± 0.01</b>	2.87 ± 0.04	7.03 ± 0.04
Bone age	NN	NA	NA	18.68
	QD	0.90	<b>1.99</b>	20.24
	QD+	<b>1.00</b>	5.24	25.18
	DE	<b>0.93</b>	2.17	18.69
	PIVEN	<b>0.93</b>	2.09	<b>18.13</b>

## 5.6 UCI Datasets Results

We evaluate the UCI datasets with  $\alpha = 0.05$ , as done in previous works, with additional experiments later in this section. Since all methods achieved the required PICP metric, we present these results in Table 8 in the appendix. The results for the MPIW and RMSE metrics are presented in Table 2. In terms of PI-quality, PIVEN achieves top performance eight of of ten datasets (QD achieves

Table 2: Regression results for benchmark UCI datasets comparing MPIW, and RMSE. The grey column contains the results for QD+ with their proposed aggregation method, as reported by the authors.

Datasets	MPIW					RMSE				
	DE	QD	QD+	PIVEN	QD+(Reported)	DE	QD	QD+	PIVEN	QD+(Reported)
Boston	<b>0.87 ± 0.03</b>	1.15 ± 0.02	4.98 ± 0.81	1.09 ± 0.01	1.58 ± 0.06	<b>2.87 ± 0.19</b>	3.39 ± 0.26	6.12 ± 0.73	3.13 ± 0.21	0.12 ± 0.01
Concrete	<b>1.01 ± 0.02</b>	1.08 ± 0.01	3.43 ± 0.26	1.02 ± 0.01	0.99 ± 0.04	<b>5.21 ± 0.09</b>	5.88 ± 0.10	11.87 ± 0.83	5.43 ± 0.13	0.05 ± 0.00
Energy	0.49 ± 0.01	0.45 ± 0.01	1.52 ± 0.18	<b>0.42 ± 0.01</b>	0.29 ± 0.01	1.68 ± 0.06	2.28 ± 0.04	7.05 ± 0.56	<b>1.65 ± 0.03</b>	0.00 ± 0.00
Kin8nm	1.14 ± 0.01	1.18 ± 0.00	2.64 ± 0.19	<b>1.10 ± 0.00</b>	1.07 ± 0.01	0.08 ± 0.00	0.08 ± 0.00	0.19 ± 0.01	<b>0.07 ± 0.00</b>	0.06 ± 0.00
Naval	0.31 ± 0.01	0.27 ± 0.00	2.85 ± 0.15	<b>0.24 ± 0.00</b>	0.09 ± 0.00	<b>0.00 ± 0.00</b>	<b>0.00 ± 0.00</b>	0.01 ± 0.00	<b>0.00 ± 0.00</b>	0.00 ± 0.00
Power	0.91 ± 0.00	<b>0.86 ± 0.00</b>	1.51 ± 0.06	<b>0.86 ± 0.00</b>	0.80 ± 0.00	<b>3.99 ± 0.04</b>	4.14 ± 0.04	12.00 ± 0.61	4.08 ± 0.04	0.05 ± 0.00
Protein	2.68 ± 0.01	<b>2.27 ± 0.01</b>	3.30 ± 0.03	<b>2.26 ± 0.01</b>	2.12 ± 0.01	<b>4.36 ± 0.02</b>	4.99 ± 0.02	5.10 ± 0.09	<b>4.35 ± 0.02</b>	0.36 ± 0.00
Wine	2.50 ± 0.02	<b>2.24 ± 0.02</b>	4.89 ± 0.12	<b>2.22 ± 0.01</b>	2.62 ± 0.06	<b>0.62 ± 0.01</b>	0.67 ± 0.01	0.70 ± 0.04	<b>0.63 ± 0.01</b>	0.62 ± 0.02
Yacht	0.33 ± 0.02	0.18 ± 0.00	1.25 ± 0.23	<b>0.17 ± 0.00</b>	0.12 ± 0.00	1.38 ± 0.07	1.10 ± 0.06	8.19 ± 1.26	<b>0.98 ± 0.07</b>	0.00 ± 0.00
MSD	2.91 ± NA	2.45 ± NA	4.25 ± NA	<b>2.42 ± NA</b>	2.34 ± NA	8.95 ± NA	9.30 ± NA	10.11 ± 0.00	<b>8.93 ± NA</b>	0.64 ± NA

comparable results in three), while achieving comparable performance to DE in one of the remaining datasets. For the RMSE metric, it is clear that PIVEN and DE are the top performers, with the former achieving the best results in five datasets, and the latter in four. These results are notable because DE does not need to simultaneously optimize for PI and value prediction, while PIVEN aims to balance these two goals. The QD and QD+ baselines trail behind the other methods in all datasets but one. QD’s performance is not surprising given that the focus of this approach is PI generation rather than value prediction, and QD+’s need to optimize a larger number of terms in the loss function. Finally, we also perform additional experiments for DE with ensemble size  $M = 1$ , with the results presented in the appendix (Table 7).

For completeness, we also include the results of QD+ with their proposed aggregation method, as reported in [29]. These results appear as QD+(reported) in Table 2. The large difference in performance between the two QD+ variants leads us to conclude that QD+’s multiple terms in the loss function increase model complexity, which in turn makes their computationally-heavy optimization necessary. Using this optimization, however, makes QD+ impractical for large datasets. This conclusion is supported by the authors of [29]: “A potential drawback of SNM is the apparent computational overhead of fitting the split normal mixture when the number of samples is large”.

**Performance in varying levels of coverage.** In Section 3.2 we hypothesize that PIVEN’s auxiliary head makes it less prone to overfitting by enabling it to train on the entire training set rather than only on the data points captured within their PIs, as done by current SOTA PI-based approaches such as QD. To test this hypothesis, we evaluate PIVEN and QD on varying levels of coverage, i.e., where we require different percentages of the dataset to be captured by their PIs. Summary results for MPIW are presented in Table 3 and full results are in Appendix D. It is clear that as coverage decreases, PIVEN’s relative performance to QD improves. While PIVEN’s advantage is more pronounced in lower coverage rates, it persists in all coverage levels. Next, we compare the two methods using the RMSE metric. The results of our analysis – an example of which is presented in Figure 3 and the full results in Appendix D – clearly show that while QD’s performance deteriorates along with the coverage levels, PIVEN’s remains largely unchanged.

Datasets	alpha					
	0.05	0.10	0.15	0.20	0.25	0.30
Boston	7%	7%	6%	7%	8%	8%
Concrete	7%	7%	8%	7%	12%	13%
Energy	6%	12%	8%	17%	19%	27%
Kin8nm	5%	7%	9%	19%	13%	15%
Naval	10%	16%	16%	14%	17%	23%
Power	0%	0%	1%	1%	1%	1%
Protein	1%	1%	2%	3%	2%	2%
Wine	0%	1%	2%	2%	4%	4%
Yacht	8%	12%	14%	20%	20%	21%
MSD	1%	-3%	-3%	1%	-5%	-2%
<b>Average</b>	<b>4.5%</b>	<b>6.0%</b>	<b>6.3%</b>	<b>9.1%</b>	<b>9.1%</b>	<b>11.2%</b>

Table 3: MPIW improvement in percentages (PIVEN relative to QD) as the coverage decreases (i.e, alpha increases).

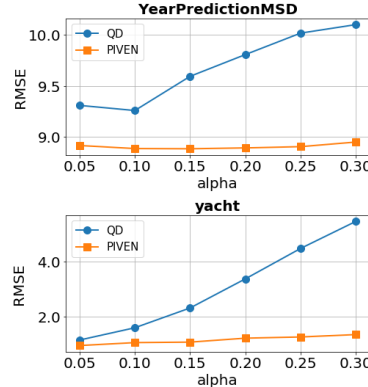


Figure 3: RMSE as function of  $\alpha$  on two of the UCI datasets. See Appendix D for full results.



## 6 Analysis

### 6.1 Auxiliary Head Analysis

In Section 3.2 we describe our rationale in expressing the value prediction as a function of the upper and lower bounds of the interval. To further explore the benefits of our auxiliary head  $v$ , we evaluate two variants of PIVEN. In the first variant, denoted as POO (point-only optimization), we decouple the value prediction from the PI. The loss function of this variant is  $\mathcal{L}_{PI} + \ell(v, y_{true})$  where  $\ell$  is set to be MSE loss. In doing so, we compare PIVEN to an approach where the value prediction is not expressed as a function of the bounds (as was done in QD+ [29]). In the second variant, denoted MOI (middle of interval), the value prediction produced by the model is always the middle of the PI (in other words,  $v$  is set to 0.5). While both return the middle of the PI as value prediction, MOI differs from QD by an additional component in its loss function.

The results of our analysis are presented in Table 4, which contains the results of the MPIW and RMSE metrics (PICP values are identical, see Appendix B). The full PIVEN significantly outperforms the two other variants. We therefore conclude that both novel aspects of our approach—the simultaneous optimization of PI-width and RMSE, and the ability to select any value on the PI as the value prediction—contribute to PIVEN’s performance. Finally, note that while inferior to PIVEN, both POO and MOI outperform the QD baseline in terms of MPIW, while being equal or better for RMSE.

Table 4: Analysis comparing MPIW and RMSE. Results were analyzed as in Table 2.

Datasets	MPIW			RMSE		
	POO	MOI	PIVEN	POO	MOI	PIVEN
Boston	<b>1.09 ± 0.02</b>	1.15 ± 0.02	<b>1.09 ± 0.01</b>	3.21 ± 0.24	3.39 ± 0.27	<b>3.13 ± 0.21</b>
Concrete	<b>1.02 ± 0.01</b>	1.07 ± 0.01	<b>1.02 ± 0.01</b>	5.55 ± 0.11	5.73 ± 0.10	<b>5.43 ± 0.13</b>
Energy	<b>0.42 ± 0.01</b>	0.45 ± 0.01	<b>0.42 ± 0.01</b>	2.16 ± 0.04	2.27 ± 0.04	<b>1.65 ± 0.03</b>
Kin8nm	1.13 ± 0.00	1.17 ± 0.00	<b>1.10 ± 0.00</b>	0.08 ± 0.00	0.08 ± 0.00	<b>0.07 ± 0.00</b>
Naval	<b>0.24 ± 0.00</b>	0.30 ± 0.02	<b>0.24 ± 0.00</b>	<b>0.00 ± 0.00</b>	<b>0.00 ± 0.00</b>	<b>0.00 ± 0.00</b>
Power	<b>0.86 ± 0.00</b>	<b>0.86 ± 0.00</b>	<b>0.86 ± 0.00</b>	4.13 ± 0.04	4.15 ± 0.04	<b>4.08 ± 0.04</b>
Protein	<b>2.25 ± 0.01</b>	2.27 ± 0.01	<b>2.26 ± 0.01</b>	4.78 ± 0.02	4.99 ± 0.01	<b>4.35 ± 0.02</b>
Wine	2.24 ± 0.01	2.23 ± 0.01	<b>2.22 ± 0.01</b>	0.64 ± 0.01	0.67 ± 0.01	<b>0.63 ± 0.01</b>
Yacht	0.18 ± 0.00	0.19 ± 0.01	<b>0.17 ± 0.00</b>	0.99 ± 0.07	1.15 ± 0.08	<b>0.98 ± 0.07</b>
MSD	<b>2.42 ± NA</b>	2.43 ± NA	<b>2.42 ± NA</b>	9.10 ± NA	9.25 ± NA	<b>8.93 ± NA</b>

### 6.2 Hyperparameters Analysis

Two parameters govern the behavior of our approach:  $\beta$  (Equation 8) and  $\lambda$  (Equation 6). We use the Sine function, whose value fluctuations are challenging to any PI-producing approach, and will therefore make identifying relevant patterns easier.  $\beta$  balances the two goals of our approach: narrow PIs and accurate value predictions. As shown in Equation 8,  $\beta$  determines the weight assigned to each goal in PIVEN’s loss function. Therefore, for large values of  $\beta$  we expect PIVEN to put greater emphasis on optimizing the PI at the expense of the value prediction. For small values of  $\beta$ , we expect the opposite. Figure 4 (Left) confirms our expectations. It is clear that  $\beta = 0.99$  produces the most accurate PIs, but its value predictions is the least accurate. The opposite applies for  $\beta = 0.1$  This analysis also shows that  $\beta = 0.5$  strikes a better balance, as it optimizes for both tasks simultaneously.

The goal of  $\lambda$  is to balance capturing as many samples as possible within our PIs (PICP) with the conflicting goal of producing tight PIs (MPIW). We expect that for small  $\lambda$  values, PIVEN will attempt to produce tight PIs with less emphasis on coverage. For large  $\lambda$  values, we expect the opposite. Results in Figure 4 (Right) confirm our expectations.

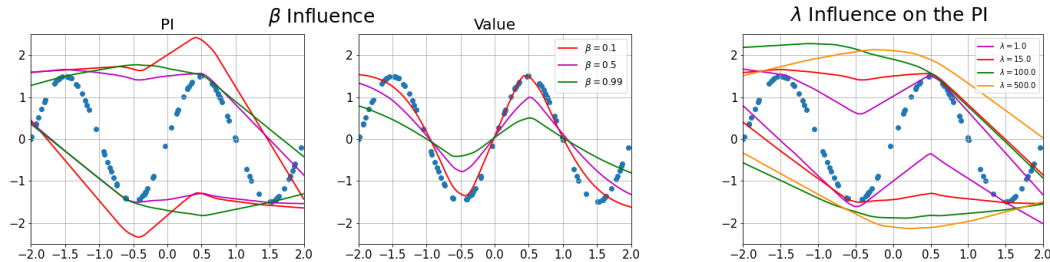


Figure 4: (Left) An analysis of the effect of varying  $\beta$  values on PIVEN’s performance in terms of PI width and value prediction. (Right) The effect of various  $\lambda$  values on the tightness of the PI

## 7 Conclusions

PIVEN is a novel architecture for combining the generation of prediction intervals together with specific value predictions in an end-to-end manner. PIVEN optimizes these two goals simultaneously and is able to achieve improved results in both. Our performance is enhanced by two factors: first, its value-prediction and PI-prediction are connected and optimized simultaneously. Secondly, PIVEN does not ignore but rather trains on data points that are not captured by the PI.

## References

- [1] Martín Abadi, Paul Barham, Jianmin Chen, Zhifeng Chen, Andy Davis, Jeffrey Dean, Matthieu Devin, Sanjay Ghemawat, Geoffrey Irving, Michael Isard, et al. Tensorflow: A system for large-scale machine learning. In *12th {USENIX} Symposium on Operating Systems Design and Implementation ({OSDI} 16)*, pages 265–283, 2016.
- [2] Mariusz Bojarski, Davide Del Testa, Daniel Dworakowski, Bernhard Firner, Beat Flepp, Praseon Goyal, Lawrence D Jackel, Mathew Monfort, Urs Muller, Jiakai Zhang, et al. End to end learning for self-driving cars. *arXiv preprint arXiv:1604.07316*, 2016.
- [3] Yarin Gal and Zoubin Ghahramani. Dropout as a bayesian approximation: Representing model uncertainty in deep learning. In *international conference on machine learning*, pages 1050–1059, 2016.
- [4] Yonatan Geifman, Guy Uziel, and Ran El-Yaniv. Bias-reduced uncertainty estimation for deep neural classifiers. *arXiv preprint arXiv:1805.08206*, 2018.
- [5] Safwan S Halabi, Luciano M Prevedello, Jayashree Kalpathy-Cramer, Artem B Mamonov, Alexander Bilbily, Mark Cicero, Ian Pan, Lucas Araújo Pereira, Rafael Teixeira Sousa, Nitamar Abdala, et al. The rsna pediatric bone age machine learning challenge. *Radiology*, 290(2):498–503, 2019.
- [6] Bobby He, Balaji Lakshminarayanan, and Yee Whye Teh. Bayesian deep ensembles via the neural tangent kernel. *Advances in Neural Information Processing Systems*, 33, 2020.
- [7] James Hensman, Nicolo Fusi, and Neil D Lawrence. Gaussian processes for big data. *arXiv preprint arXiv:1309.6835*, 2013.
- [8] José Miguel Hernández-Lobato and Ryan Adams. Probabilistic backpropagation for scalable learning of bayesian neural networks. In *International Conference on Machine Learning*, pages 1861–1869, 2015.
- [9] Gao Huang, Zhuang Liu, Laurens Van Der Maaten, and Kilian Q Weinberger. Densely connected convolutional networks. In *Proceedings of the IEEE conference on computer vision and pattern recognition*, pages 4700–4708, 2017.
- [10] Sergey Ioffe and Christian Szegedy. Batch normalization: Accelerating deep network training by reducing internal covariate shift. *arXiv preprint arXiv:1502.03167*, 2015.
- [11] Elia Kaufmann, Antonio Loquercio, Rene Ranftl, Alexey Dosovitskiy, Vladlen Koltun, and Davide Scaramuzza. Deep drone racing: Learning agile flight in dynamic environments. *arXiv preprint arXiv:1806.08548*, 2018.
- [12] Alex Kendall and Yarin Gal. What uncertainties do we need in bayesian deep learning for computer vision? In *Advances in neural information processing systems*, pages 5574–5584, 2017.
- [13] Gil Keren, Nicholas Cummins, and Björn Schuller. Calibrated prediction intervals for neural network regressors. *IEEE Access*, 6:54033–54041, 2018.

- [14] Abbas Khosravi, Saeid Nahavandi, Doug Creighton, and Amir F Atiya. Lower upper bound estimation method for construction of neural network-based prediction intervals. *IEEE transactions on neural networks*, 22(3):337–346, 2010.
- [15] Diederik P Kingma and Jimmy Ba. Adam: A method for stochastic optimization. *arXiv preprint arXiv:1412.6980*, 2014.
- [16] Danijel Kivaranovic, Kory D Johnson, and Hannes Leeb. Adaptive, distribution-free prediction intervals for deep neural networks. *arXiv preprint arXiv:1905.10634*, 2019.
- [17] Balaji Lakshminarayanan, Alexander Pritzel, and Charles Blundell. Simple and scalable predictive uncertainty estimation using deep ensembles. In *Advances in neural information processing systems*, pages 6402–6413, 2017.
- [18] David JC MacKay. A practical bayesian framework for backpropagation networks. *Neural computation*, 4(3):448–472, 1992.
- [19] Vinod Nair and Geoffrey E Hinton. Rectified linear units improve restricted boltzmann machines. In *Proceedings of the 27th international conference on machine learning (ICML-10)*, pages 807–814, 2010.
- [20] David A Nix and Andreas S Weigend. Estimating the mean and variance of the target probability distribution. In *Proceedings of 1994 IEEE international conference on neural networks (ICNN'94)*, volume 1, pages 55–60. IEEE, 1994.
- [21] Khusnul Novianingsih and Rieske Hadianiti. Modeling flight departure delay distributions. In *2014 International Conference on Computer, Control, Informatics and Its Applications (IC3INA)*, pages 30–34. IEEE, 2014.
- [22] Yaniv Ovadia, Emily Fertig, Jie Ren, Zachary Nado, David Sculley, Sebastian Nowozin, Joshua Dillon, Balaji Lakshminarayanan, and Jasper Snoek. Can you trust your model’s uncertainty? evaluating predictive uncertainty under dataset shift. In *Advances in Neural Information Processing Systems*, pages 13991–14002, 2019.
- [23] Tim Pearce, Mohamed Zaki, Alexandra Brintrup, and Andy Neely. High-quality prediction intervals for deep learning: A distribution-free, ensembled approach. *arXiv preprint arXiv:1802.07167*, 2018.
- [24] Florian A Potra and Stephen J Wright. Interior-point methods. *Journal of Computational and Applied Mathematics*, 124(1-2):281–302, 2000.
- [25] Xin Qiu, Elliot Meyerson, and Risto Miikkulainen. Quantifying point-prediction uncertainty in neural networks via residual estimation with an i/o kernel. *arXiv preprint arXiv:1906.00588*, 2019.
- [26] Muhammad Imran Razzak, Saeeda Naz, and Ahmad Zaib. Deep learning for medical image processing: Overview, challenges and the future. In *Classification in BioApps*, pages 323–350. Springer, 2018.
- [27] Yaniv Romano, Evan Patterson, and Emmanuel Candes. Conformalized quantile regression. In *Advances in Neural Information Processing Systems*, pages 3538–3548, 2019.
- [28] Rasmus Rothe, Radu Timofte, and Luc Van Gool. Deep expectation of real and apparent age from a single image without facial landmarks. *International Journal of Computer Vision*, 126(2-4):144–157, 2018.
- [29] Tárík S Salem, Helge Langseth, and Heri Ramampiaro. Prediction intervals: Split normal mixture from quality-driven deep ensembles. In *Conference on Uncertainty in Artificial Intelligence*, pages 1179–1187. PMLR, 2020.
- [30] Karen Simonyan and Andrew Zisserman. Very deep convolutional networks for large-scale image recognition. *arXiv preprint arXiv:1409.1556*, 2014.
- [31] Nitish Srivastava, Geoffrey Hinton, Alex Krizhevsky, Ilya Sutskever, and Ruslan Salakhutdinov. Dropout: a simple way to prevent neural networks from overfitting. *The journal of machine learning research*, 15(1):1929–1958, 2014.
- [32] Natasa Tagasovska and David Lopez-Paz. Single-model uncertainties for deep learning. In *Advances in Neural Information Processing Systems*, pages 6414–6425, 2019.
- [33] Kenneth F Wallis. The two-piece normal, binormal, or double gaussian distribution: its origin and rediscoveries. *Statistical Science*, pages 106–112, 2014.
- [34] Tsun-Yi Yang, Yi-Hsuan Huang, Yen-Yu Lin, Pi-Cheng Hsiu, and Yung-Yu Chuang. Ssr-net: A compact soft stagewise regression network for age estimation. In *IJCAI*, volume 5, page 7, 2018.
- [35] Yunxuan Zhang, Li Liu, Cheng Li, et al. Quantifying facial age by posterior of age comparisons. *arXiv preprint arXiv:1708.09687*, 2017.
- [36] Lingxue Zhu and Nikolay Laptev. Deep and confident prediction for time series at uber. In *2017 IEEE International Conference on Data Mining Workshops (ICDMW)*, pages 103–110. IEEE, 2017.

## A Experimental Setup

In this section we provide full details of our dataset preprocessing and experiments presented in the main study. Our code is available online <sup>2</sup>

### A.1 Synthetic Datasets

For the qualitative training method comparison, QD vs. PIVEN (Section 5.4), all NNs used ReLU activations and 100 nodes in one hidden layer. Both methods trained until convergence using the same initialization, loss and default hyperparameters, as described in [23]:  $\alpha = 0.05$ ,  $\beta = 0.5$ ,  $\lambda = 15.0$ ,  $s = 160.0$ , and the random seed was set to 1. The generated data consisted of 100 points sampled uniformly from the interval  $[-2, 2]$ . We used  $\alpha = 100$  as the skewness parameter. In Figures 2 and 5 we present a comparison on the Sine and skewed-normal distributions.

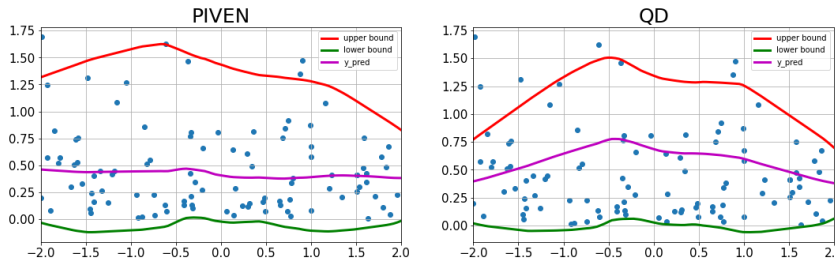


Figure 5: Value prediction comparison, where  $\mathbf{y}$  is sampled from skewed-normal distribution  $f(x; \alpha) = 2\phi(x)\Phi(\alpha \cdot x)$  where  $\phi(x)$  and  $\Phi(\alpha \cdot x)$  denote the  $\mathcal{N}(0, 1)$  density and distribution function respectively; the parameter  $\alpha$  denotes the skewness parameter.

### A.2 Dataset Preprocessing and Full Experimental Setup

In addition to the ten benchmark datasets used by all recent studies in the field, we evaluated PIVEN on two large image datasets. Due to the size of the datasets and the nature of the domain, preprocessing was required. We provide the full details of the process below.

**UCI datasets.** For the UCI datasets, we used the experimental setup proposed by [8], which was also used in all the two baselines described in this study. All datasets were averaged on 20 random splits of the data, except for the “Year Prediction MSD” and “protein” datasets. Since “Year Prediction MSD” has predefined fixed splits by the provider, only one run was conducted. For “protein”, 5 splits were used, as was done in previous work. Number of samples and features for each dataset is presented in Table 5. We used identical network architectures to those described in previous works: one dense layer with ReLU [19], containing 50 neurons for each network. In the “Year Prediction MSD” and “protein” datasets where NNs had 100 neurons. Regarding train/test split and hyperparameters, we employ the same setup as [23]: train/test folds were randomly split 90%/10%, input and target variables were normalized to zero mean and unit variance. The softening factor was constant for all datasets,  $s = 160.0$ . For the majority of the datasets we used  $\lambda = 15.0$ , except for “naval”, “protein”, “wine” and “yacht” where  $\lambda$  was set to 4.0, 40.0, 30.0 and 3.0 respectively. The value of the parameter  $\beta$  was set to 0.5. The Adam optimizer [15] was used with exponential decay, where learning rate and decay rate were tuned. Batch size of 100 was used for all the datasets, except for “Year Prediction MSD” where batch size was set to 1000. Five neural nets were used in each ensemble, using parameter re-sampling. The objective used to optimized  $v$  was Mean Square Error (MSE) for all datasets. We also tune  $\lambda$ , initializing variance, and number of training epochs using early stopping. To ensure that our comparison with the state-of-the-art baselines is accurate, we first set the parameters of our neural nets so that they produce the results reported in [23]. We then use the same parameter configurations in our experiments of PIVEN.

**IMDB age estimation dataset<sup>3</sup>.** For the IMDB dataset, we used the DenseNet architecture [9] as a feature extractor. On top of this architecture we added two dense layers with dropout. The sizes of the two dense layers were 128 and 32 neurons respectively, with a dropout factor of 0.2, and ReLU activation [19]. In the last layer, the biases of the PIs were initially set to  $[5.0, -5.0]$  for the upper and lower bounds respectively. We used the data preprocessing similar to that of previous work [34, 35]: all face images were aligned using facial landmarks such as eyes and the nose. After alignment, the face region of each image was cropped and resized to a  $64 \times 64$  resolution. In addition, common data augmentation methods, including zooming, shifting, shearing, and flipping

<sup>2</sup><https://github.com/anonymous/anonymous>

<sup>3</sup><https://data.vision.ee.ethz.ch/cvl/rrothe/imdb-wiki/>

Table 5: Number of samples and features for UCI datasets

Dataset	# samples	# features
Boston	506	14
Concrete	1030	9
Energy	768	9
Kin8nm	8192	9
Naval	11934	18
Power	9568	5
Protein	45730	10
Wine	1599	12
Yacht	308	7
MSD	515345	90

were randomly activated. The Adam optimization method [15] was used for optimizing the network parameters over 90 epochs, with a batch size of 128. The learning rate was set to 0.002 initially and reduced by a factor 0.1 every 30 epochs. Regarding loss hyperparameters, we used the standard configuration proposed in [23]: confidence interval set to 0.95, soften factor set to 160.0 and  $\lambda = 15.0$ . For PIVEN we used the same setting, with  $\beta = 0.1$ . Since there was no predefined test set for this dataset, we employed a 5-fold cross validation: In each split, we used 20% as the test set. Additionally, 20% of the train set was designated as the validation set. Best model obtained by minimizing the validation loss. In QD and PIVEN, we normalized ages to zero mean and unit variance.

**RSNA pediatric bone age dataset**<sup>4</sup>. For the RSNA dataset, we used the well-known VGG-16 architecture [30] as a base model, with weights pre-trained on ImageNet. On top of this architecture, we added batch normalization [10], attention mechanism with two CNN layers of 64 and 16 neurons each, two average pooling layers, dropout [31] with a 0.25 probability, and a fully connected layer with 1024 neurons. The activation function for the CNN layers was ReLU [19], and we used ELU for the fully connected layer. For the PIs last layer, we used biases of  $[2.0, -2.0]$ , for the upper and lower bound initialization, respectively. We used standard data augmentation consisting of horizontal flips, vertical and horizontal shifts, and rotations. In addition, we normalized targets to zero mean and unit variance. To reduce computational costs, we downscaled input images to  $384 \times 384$  pixels. The network was optimized using Adam optimizer [15], with an initial learning rate of 0.01 which was reduced when the validation loss has stopped improving over 10 epochs. We trained the network for 50 epochs using batch size of 100. For our loss hyperparameters, we used the standard configuration like proposed in [23]: confidence interval set to 0.95, soften factor set to 160.0 and  $\lambda = 15.0$ . For PIVEN, we used the same setting, with  $\beta = 0.5$ .

---

<sup>4</sup><https://www.kaggle.com/kmader/rsna-bone-age>

## B UCI Analysis full results

In Table 6 we present the full results of our ablation studies, including PICP, for the ablation variants.

Table 6: Ablation analysis, comparing PICP, MPIW and RMSE. The guidelines for selecting best results are as those used in Table 2.

Datasets	PICP			MPIW			RMSE		
	POO	MOI	PIVEN	POO	MOI	PIVEN	POO	MOI	PIVEN
Boston	<b>0.93 ± 0.01</b>	<b>0.93 ± 0.01</b>	<b>0.93 ± 0.01</b>	<b>1.09 ± 0.02</b>	1.15 ± 0.02	<b>1.09 ± 0.01</b>	3.21 ± 0.24	3.39 ± 0.27	<b>3.13 ± 0.21</b>
Concrete	<b>0.93 ± 0.01</b>	<b>0.93 ± 0.01</b>	<b>0.93 ± 0.01</b>	<b>1.02 ± 0.01</b>	1.07 ± 0.01	<b>1.02 ± 0.01</b>	5.55 ± 0.11	5.73 ± 0.10	<b>5.43 ± 0.13</b>
Energy	<b>0.97 ± 0.01</b>	<b>0.97 ± 0.00</b>	<b>0.97 ± 0.00</b>	<b>0.42 ± 0.01</b>	0.45 ± 0.01	<b>0.42 ± 0.01</b>	2.16 ± 0.04	2.27 ± 0.04	<b>1.65 ± 0.03</b>
Kin8nm	<b>0.96 ± 0.00</b>	<b>0.96 ± 0.00</b>	<b>0.96 ± 0.00</b>	1.13 ± 0.00	1.17 ± 0.00	<b>1.10 ± 0.00</b>	0.08 ± 0.00	0.08 ± 0.00	<b>0.07 ± 0.00</b>
Naval	<b>0.98 ± 0.00</b>	<b>0.98 ± 0.00</b>	<b>0.98 ± 0.00</b>	<b>0.24 ± 0.00</b>	0.30 ± 0.02	<b>0.24 ± 0.00</b>	<b>0.00 ± 0.00</b>	<b>0.00 ± 0.00</b>	<b>0.00 ± 0.00</b>
Power	<b>0.96 ± 0.00</b>	<b>0.96 ± 0.00</b>	<b>0.96 ± 0.00</b>	<b>0.86 ± 0.00</b>	<b>0.86 ± 0.00</b>	<b>0.86 ± 0.00</b>	4.13 ± 0.04	4.15 ± 0.04	<b>4.08 ± 0.04</b>
Protein	<b>0.95 ± 0.00</b>	<b>0.95 ± 0.00</b>	<b>0.95 ± 0.00</b>	<b>2.25 ± 0.01</b>	2.27 ± 0.01	<b>2.26 ± 0.01</b>	4.78 ± 0.02	4.99 ± 0.01	<b>4.35 ± 0.02</b>
Wine	<b>0.91 ± 0.01</b>	<b>0.91 ± 0.01</b>	<b>0.91 ± 0.01</b>	2.24 ± 0.01	2.23 ± 0.01	<b>2.22 ± 0.01</b>	0.64 ± 0.01	0.67 ± 0.01	<b>0.63 ± 0.01</b>
Yacht	<b>0.95 ± 0.01</b>	<b>0.95 ± 0.01</b>	<b>0.95 ± 0.01</b>	0.18 ± 0.00	0.19 ± 0.01	<b>0.17 ± 0.00</b>	0.99 ± 0.07	1.15 ± 0.08	<b>0.98 ± 0.07</b>
MSD	<b>0.95 ± NA</b>	<b>0.95 ± NA</b>	<b>0.95 ± NA</b>	<b>2.42 ± NA</b>	2.43 ± NA	<b>2.42 ± NA</b>	9.10 ± NA	9.25 ± NA	<b>8.93 ± NA</b>

Additionally, we tested the Deep Ensembles baseline with an ensemble size of one. We expect the baseline to under-perform in this setting, and this expectation is supported by the results presented in Table 7.

Table 7: Results on regression benchmark UCI datasets comparing PICP, MPIW, and RMSE. The guidelines for selecting best results are as those used in Table 2. Note: the results for DE are presented for ensemble size of one, denotes as *DE-One*.

Datasets	DE-One	PICP			DE-One	MPIW			DE-One	RMSE		
		QD	PIVEN	PIVEN		QD	PIVEN	PIVEN		QD	PIVEN	PIVEN
Boston	0.76 ± 0.01	<b>0.93 ± 0.01</b>	<b>0.93 ± 0.01</b>	<b>0.93 ± 0.01</b>	0.75 ± 0.02	1.15 ± 0.02	1.09 ± 0.01	<b>3.11 ± 0.21</b>	3.39 ± 0.26	3.13 ± 0.21		
Concrete	0.87 ± 0.01	<b>0.93 ± 0.01</b>	<b>0.93 ± 0.01</b>	<b>0.93 ± 0.01</b>	0.93 ± 0.02	1.08 ± 0.01	1.02 ± 0.01	5.52 ± 0.13	5.88 ± 0.10	<b>5.43 ± 0.13</b>		
Energy	0.93 ± 0.01	<b>0.97 ± 0.01</b>	<b>0.97 ± 0.01</b>	<b>0.97 ± 0.00</b>	0.43 ± 0.02	0.45 ± 0.01	<b>0.42 ± 0.01</b>	1.72 ± 0.06	2.28 ± 0.04	<b>1.65 ± 0.05</b>		
Kin8nm	0.93 ± 0.00	<b>0.96 ± 0.00</b>	<b>0.96 ± 0.00</b>	<b>0.96 ± 0.00</b>	1.06 ± 0.01	1.18 ± 0.00	<b>1.10 ± 0.00</b>	0.08 ± 0.00	0.08 ± 0.00	<b>0.07 ± 0.00</b>		
Naval	0.94 ± 0.00	<b>0.97 ± 0.00</b>	<b>0.97 ± 0.00</b>	<b>0.98 ± 0.00</b>	0.25 ± 0.01	0.27 ± 0.00	<b>0.24 ± 0.00</b>	<b>0.00 ± 0.00</b>	<b>0.00 ± 0.00</b>	<b>0.00 ± 0.00</b>		
Power	<b>0.96 ± 0.00</b>	<b>0.96 ± 0.00</b>	<b>0.96 ± 0.00</b>	<b>0.96 ± 0.00</b>	0.90 ± 0.00	<b>0.86 ± 0.00</b>	<b>0.86 ± 0.00</b>	<b>4.01 ± 0.04</b>	4.14 ± 0.04	4.08 ± 0.04		
Protein	<b>0.95 ± 0.00</b>	<b>0.95 ± 0.00</b>	<b>0.95 ± 0.00</b>	<b>0.95 ± 0.00</b>	2.64 ± 0.01	<b>2.27 ± 0.01</b>	<b>2.26 ± 0.01</b>	4.43 ± 0.02	4.99 ± 0.02	<b>4.35 ± 0.02</b>		
Wine	0.86 ± 0.01	<b>0.91 ± 0.01</b>	<b>0.91 ± 0.01</b>	<b>0.91 ± 0.01</b>	2.34 ± 0.02	<b>2.24 ± 0.02</b>	<b>2.22 ± 0.01</b>	<b>0.64 ± 0.01</b>	0.67 ± 0.01	<b>0.63 ± 0.01</b>		
Yacht	<b>0.95 ± 0.01</b>	<b>0.95 ± 0.01</b>	<b>0.95 ± 0.01</b>	<b>0.95 ± 0.01</b>	0.26 ± 0.02	0.18 ± 0.00	<b>0.17 ± 0.00</b>	1.42 ± 0.07	1.10 ± 0.06	<b>0.98 ± 0.07</b>		
MSD	<b>0.95 ± NA</b>	<b>0.95 ± NA</b>	<b>0.95 ± NA</b>	<b>0.95 ± NA</b>	2.86 ± NA	2.45 ± NA	<b>2.42 ± NA</b>	9.03 ± NA	9.30 ± NA	<b>8.93 ± NA</b>		

Table 8: an extension of Table 2 evaluating MPIW with PICP for all our baselines.

Datasets	DE	PICP				DE	MPIW			
		QD	QD+	PIVEN	PIVEN		QD	QD+	PIVEN	PIVEN
Boston	0.87 ± 0.01	<b>0.93 ± 0.01</b>	<b>1.00 ± 0.01</b>	<b>0.93 ± 0.01</b>	0.87 ± 0.03	1.15 ± 0.02	4.98 ± 0.81	1.09 ± 0.01		
Concrete	0.92 ± 0.01	<b>0.93 ± 0.01</b>	<b>1.00 ± 0.01</b>	<b>0.93 ± 0.01</b>	1.01 ± 0.02	1.08 ± 0.01	3.43 ± 0.26	1.02 ± 0.01		
Energy	<b>0.99 ± 0.00</b>	<b>0.97 ± 0.01</b>	<b>0.99 ± 0.01</b>	<b>0.97 ± 0.00</b>	0.49 ± 0.01	0.45 ± 0.01	1.52 ± 0.18	<b>0.42 ± 0.01</b>		
Kin8nm	<b>0.97 ± 0.00</b>	<b>0.96 ± 0.00</b>	<b>0.99 ± 0.00</b>	<b>0.96 ± 0.00</b>	1.14 ± 0.01	1.18 ± 0.00	2.64 ± 0.19	<b>1.10 ± 0.00</b>		
Naval	<b>0.98 ± 0.00</b>	<b>0.97 ± 0.00</b>	<b>0.99 ± 0.01</b>	<b>0.98 ± 0.00</b>	0.31 ± 0.01	0.27 ± 0.00	2.85 ± 0.15	<b>0.24 ± 0.00</b>		
Power	<b>0.96 ± 0.00</b>	<b>0.96 ± 0.00</b>	<b>0.99 ± 0.00</b>	<b>0.96 ± 0.00</b>	0.91 ± 0.00	<b>0.86 ± 0.00</b>	1.51 ± 0.06	<b>0.86 ± 0.00</b>		
Protein	<b>0.96 ± 0.00</b>	<b>0.95 ± 0.00</b>	<b>0.99 ± 0.00</b>	<b>0.95 ± 0.00</b>	2.68 ± 0.01	<b>2.27 ± 0.01</b>	3.30 ± 0.03	<b>2.26 ± 0.01</b>		
Wine	0.90 ± 0.01	<b>0.91 ± 0.01</b>	<b>1.00 ± 0.00</b>	<b>0.91 ± 0.01</b>	2.50 ± 0.02	<b>2.24 ± 0.02</b>	4.89 ± 0.12	<b>2.22 ± 0.01</b>		
Yacht	<b>0.98 ± 0.01</b>	<b>0.95 ± 0.01</b>	<b>0.97 ± 0.03</b>	<b>0.95 ± 0.01</b>	0.33 ± 0.02	0.18 ± 0.00	1.25 ± 0.23	<b>0.17 ± 0.00</b>		
MSD	<b>0.95 ± NA</b>	<b>0.95 ± NA</b>	<b>0.99 ± NA</b>	<b>0.95 ± NA</b>	2.91 ± NA	2.45 ± NA	4.25 ± NA	<b>2.42 ± NA</b>		

## C Evaluation under Dataset Shift

Dataset shift is a challenging problem in which the dataset composition and/or distribution changes over time. This scenario poses significant challenges to the application of machine learning algorithms, because these models tend to assume similar distributions between their train and test sets. Dataset shift scenarios are of particular interest to uncertainty modeling [22], as it enables researchers to evaluate algorithms’ robustness and adaptability. We now evaluate PIVEN’s ability to adjust to this challenging scenario.

For our evaluation, we chose the Flight Delays dataset [7], which is known to contain dataset shift. We train PIVEN and our baselines on the first 700K data points and test on the next 100K test points at 5 different starting points: 700K, 2M (million), 3M, 4M and 5M. This experimental setting *fully replicates* (both in terms of dataset splits and the neural architectures used in the experiments) the one presented in [6]. The dataset is ordered chronologically throughout the year 2008, and it is evident that the dataset shift increases over time. Our

experimental results – using the PICP, MPIW and RMSE metrics – are presented in Figure 6. As in our other experiments, we present the results for a confidence level of 95% (i.e.  $\alpha = 0.05$ ).

The results show that PIVEN outperforms the baselines in MPIW metric (a result consistent with our other experiments) while achieving the desired coverage rate. Interestingly, our approach is also competitive in terms of the RMSE metric, although the value fluctuations make it difficult to reach a clear conclusion. Neither approach reached the desired PICP level in the first test set, but all were able to do so in consequent experiments. DE was able to achieve slightly higher PICP rates than the other two methods, but its PI width were larger than the other two methods. In contrast, PIVEN manages to achieve the desired PICP levels while producing smaller intervals. It should be noted that the dataset exhibits seasonal effect between 2M and 3M samples, which causes variance in performance. This phenomenon is described in [6]. We hypothesize that the reason PIVEN outperforms DE in terms of PI width is due to the fact that the former aims to optimize MPIW, whereas DE aims to optimize for negative log-likelihood [17]. Additionally, the Flight Delays dataset is known to have a non-Gaussian distribution [21] which invalidates the basic assumption applied by DE.

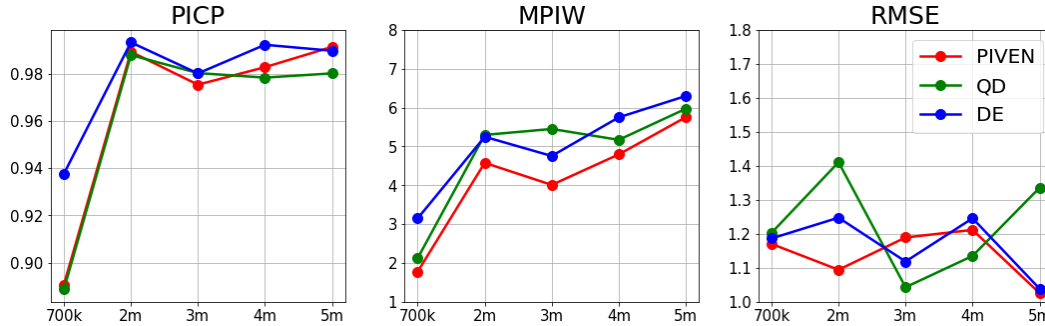


Figure 6: Comparison between PIVEN and the baselines in terms of PICP (left), MPIW (center) and RMSE (right) for  $\alpha = 0.05$ .

## D Full Results - PI Performance as a Function of Coverage

We argue that QD only focuses on the fraction  $c$  of the training set which was successfully captured by the PI. In this experiment we study the effect of changes in the coverage levels (represented by  $\alpha$ ) on the width of the PI produced both by PIVEN and QD. Additionally, we examine the affect of  $\alpha$  on the value prediction. In Figures 7, 8 and 9, we present our results – measured by PICP, MPIW and RMSE – on all UCI datasets. As expected, PIVEN consistently outperforms QD in the above metrics.

**PI Coverage.** Both methods are able to achieve the coverage desired by  $\alpha$ , which decreases as  $\alpha$  increases, as expected.

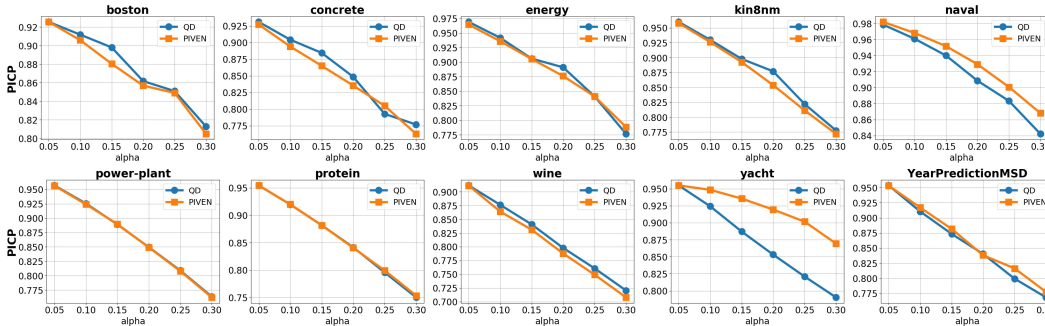


Figure 7: comparing PICP between QD and PIVEN over different values of alpha.

**PI Width.** QD’s inability to consider points outside the PI clearly degrades its performance. PIVEN, on the other hand, is able to reduce MPIW consistently over all datasets.

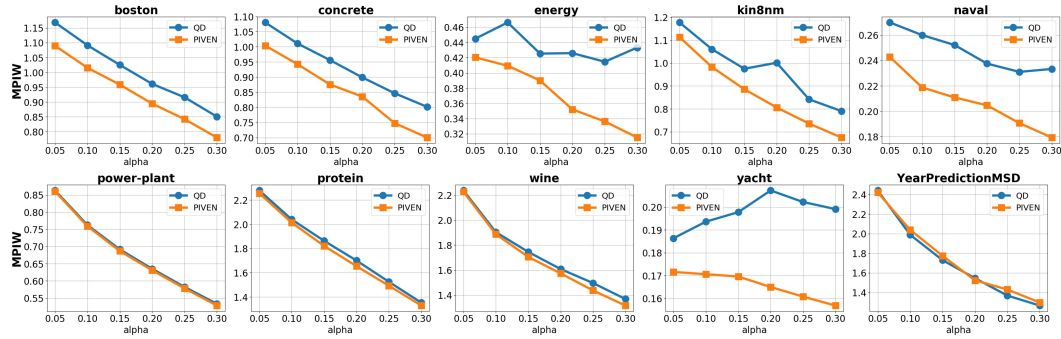


Figure 8: comparing MPIW between QD and PIVEN over different values of alpha.

**Value prediction accuracy.** Due to the way QD performs its value prediction (i.e., middle of the PI), the value prediction is not able to improve, and in fact degrades. Contrarily, PIVEN’s robustness enables it to generally maintain (with a slight decrease) its performance levels.

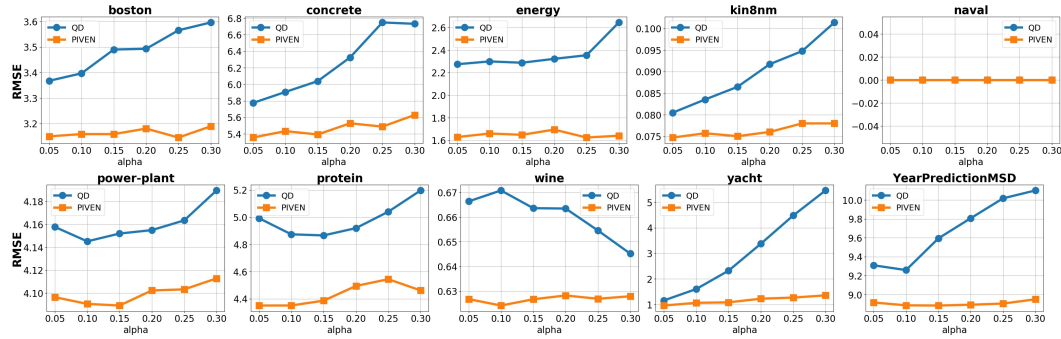


Figure 9: comparing RMSE between QD and PIVEN over different values of alpha.

## E IMDB age estimation training process and robustness to outliers

### E.1 Training process

In the following figures we present comparisons of the training progression for PIVEN, QD and NN on the MAE, PICP and MPIW evaluation metrics. We used 80% of images as the training set while the remaining 20% were used as the validation set (we did not define a test set as we were only interested in analyzing the progression of the training). For the MAE metric, presented in Figure 10, we observe that the values for QD did not improve. This is to be expected since QD does not consider this goal in its training process (i.e., loss function). This result further strengthens our argument that selecting the middle of the interval is often a sub-optimal strategy for value prediction. For the remaining two approaches – NN and PIVEN– we note that NN suffers from overfitting, given that the validation error is greater than training error after convergence. This phenomena does not happen in PIVEN which indicates robustness, a result which further supports our conclusions regarding the method’s robustness.

For the MPIW metric (Figures 11), PIVEN presents better performance both for the validation and train sets compared to QD. Moreover, we observe a smaller gap between the error produced by PIVEN for the two sets – validation and training – which indicates that PIVEN enjoys greater robustness and an ability to not overfit to a subset of the data. Our analysis also shows that for the PICP metric (Figure 12), PIVEN achieves higher levels of coverage.



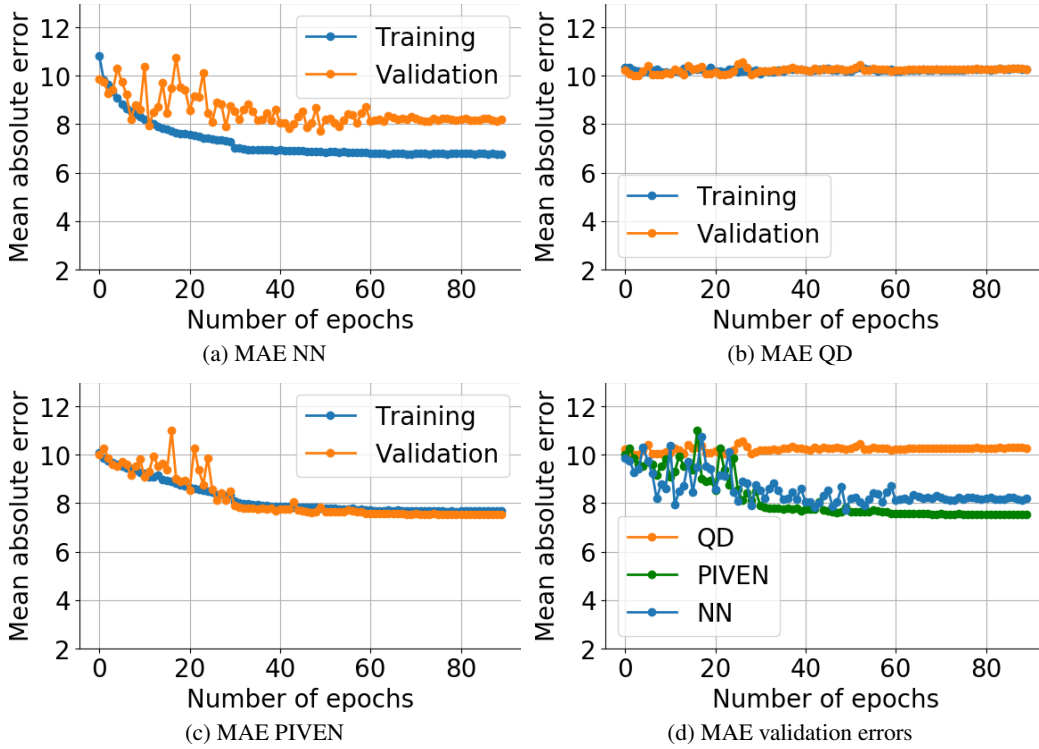


Figure 10: Comparison of MAE metric in the training process. We observe that the values for QD (b) do not improve, which is expected since QD does not consider value prediction in its loss function. Moreover, we note that NN suffers from overfitting, given that the validation error is greater than the training error after convergence. This phenomena do not affect PIVEN, thus providing an indication of its robustness.

## E.2 Robustness to outliers

Since PIVEN is capable of learning from the entire dataset while QD learns only from data points which were captured by the PI, it is reasonable to expect that the former will outperform the latter when coping with outliers. In the IMDB age estimation dataset, we can consider images with very high or very low age as outliers. Our analysis shows that for this subset of cases, there is a large gap in performance between PIVEN and QD. In Figure 13 we provide several images of very young/old individuals and the results returned by the two methods. We can observe that PIVEN copes with these outliers significantly better.

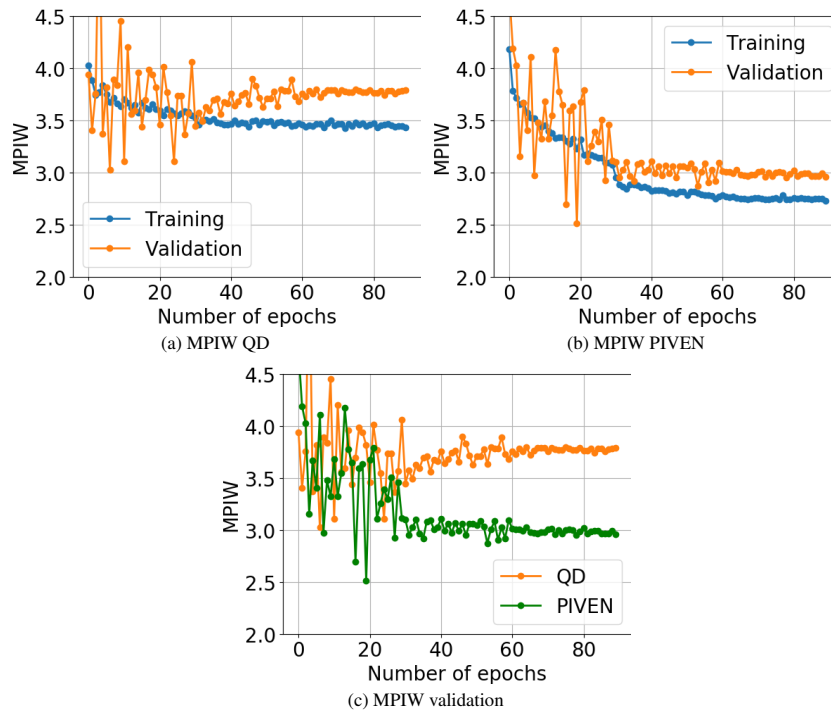


Figure 11: Comparison of the MPIW metric between QD and PIVEN in the training process. As can be seen, PIVEN significantly improves over QD, and has a smaller gap between training and validation errors.

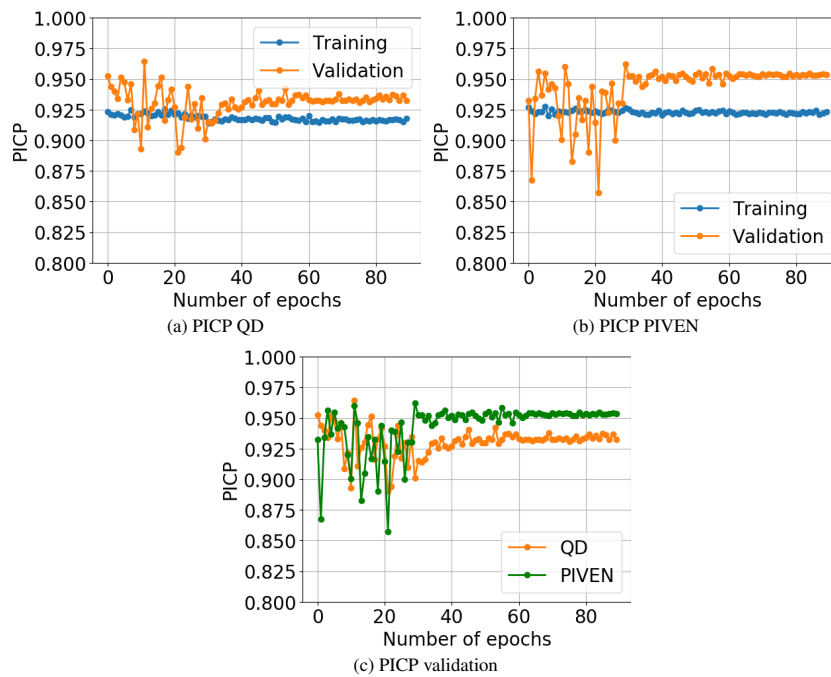


Figure 12: Comparison of PICP metric between QD and PIVEN in the training process. PIVEN achieves higher coverage when two methods converges.

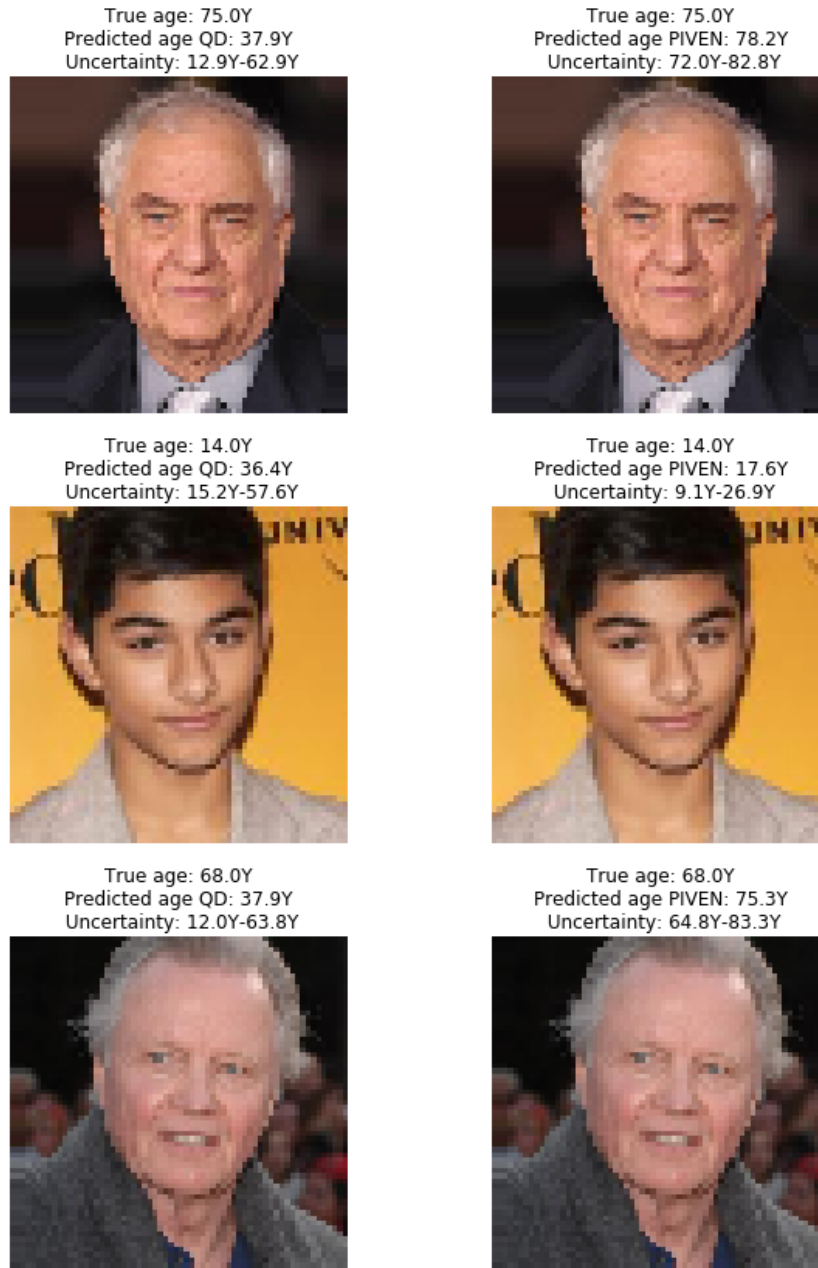


Figure 13: The predictions produced for outliers (i.e., very young/old individuals) by both PIVEN and QD for the IMDB age estimation dataset. The results for QD are on the left, results for PIVEN on the right.